bioRxiv preprint doi: https://doi.org/10.1101/2024.01.23.576890; this version posted January 24, 2024. The copyright holder for this preprint (which was not certified by peer review) is the author/funder, who has granted bioRxiv a license to display the preprint in perpetuity. It is made available under aCC-BY-NC-ND 4.0 International license.

Single-domain antibodies reveal unique borreliacidal epitopes on the Lyme disease vaccine antigen, Outer surface protein A (OspA)

David J Vance[1,2,*], Saiful Basir[2], Carol Lyn Piazza[1], Graham Willsey[1], H M Emranul Haque[3], Jacque M Tremblay[4], Michael J Rudolph[5], Beatrice Muriuki[6], Lisa A Cavacini[6], David D Weis[3,†], Charles B Shoemaker[4], and Nicholas J Mantis[1,2,*]

[1]Division of Infectious Diseases, Wadsworth Center, New York State Department of Health, Albany NY, [2]University at Albany, Department of Biomedical Sciences, Albany NY, [3]Department of Chemistry, The University of Kansas, Lawrence, KS, [4]Department of Infectious Disease and Global Health, Cummings School of Veterinary Medicine, Tufts University, North Grafton MA, [5]New York Structural Biology Center, New York, NY, [6]University of Massachusetts Chan School of Medicine, Worcester, MA

*To whom correspondence should be addressed:
David J. Vance, david.vance@health.ny.gov
Nicholas J. Mantis, nicholas.mantis@health.ny.gov

†, present address: Bristol Myers Squibb, Lawrenceville, NJ

Running Title: Nanobodies targeting the Lyme vaccine antigen, OspA

bioRxiv preprint doi: https://doi.org/10.1101/2024.01.23.576890; this version posted January 24, 2024. The copyright holder for this preprint (which was not certified by peer review) is the author/funder, who has granted bioRxiv a license to display the preprint in perpetuity. It is made available under aCC-BY-NC-ND 4.0 International license.

ABSTRACT

Camelid-derived, single-domain antibodies (V_HHs) have proven to be extremely powerful tools in defining the antigenic landscape of immunologically heterogeneous surface proteins. In this report, we generated a phage-displayed V_HH library directed against the candidate Lyme disease vaccine antigen, Outer surface protein A (OspA). Two alpacas were immunized with recombinant OspA serotype 1 (ST1) from *Borrelia burgdorferi* sensu stricto strain B31, in combination with the canine vaccine RECOMBITEK® Lyme containing lipidated OspA. The phage library was subjected to two rounds of affinity enrichment ("panning") against recombinant OspA, yielding 21 unique V_HHs within two epitope bins, as determined through competition ELISAs with a panel of OspA-specific human monoclonal antibodies. Epitope refinement was conducted by hydrogen exchange-mass spectrometry (HX-MS). Six of the monovalent V_HHs were expressed as human IgG1-Fc fusion proteins and shown to have functional properties associated with protective human monoclonal antibodies, including *B. burgdorferi* agglutination, outer membrane damage, and complement-dependent borreliacidal activity. The V_HHs displayed unique reactivity profiles with the seven OspA serotypes associated with *B. burgdorferi* genospecies in the United States and Europe consistent with there being conserved epitopes across OspA serotypes that should be considered when designing and evaluating multivalent Lyme disease vaccines.

bioRxiv preprint doi: https://doi.org/10.1101/2024.01.23.576890; this version posted January 24, 2024. The copyright holder for this preprint (which was not certified by peer review) is the author/funder, who has granted bioRxiv a license to display the preprint in perpetuity. It is made available under aCC-BY-NC-ND 4.0 International license.

INTRODUCTION

Lyme disease is the most common vector-borne infection in the United States, with an estimated 450,000 cases per year (1). The primary etiologic agent of Lyme disease in the US is the spirochetal bacterium, *Borrelia burgdorferi* sensu stricto (herein referred to as simply *B. burgdorferi*) with other genospecies responsible for disease in Europe and Asia. The spirochete is transmitted to humans by the black legged tick, *Ixodes scapularis* in the eastern US and *Ixodes pacificus* in the western part of the country. During the course a blood meal, *B. burgdorferi* migrates from the tick midgut, where it normally resides, to the salivary glands where it is deposited into the skin of a host. In humans, the spirochete proliferates at the site of the tick bite, typically resulting in an expanding skin lesion commonly referred to as a bull's eye rash or erythema migrans (2, 3). In the absence of antibiotic intervention, *B. burgdorferi* disseminates to peripheral tissues, organs, large joints, and central nervous system, potentially resulting in severe complications including neuroborreliosis, carditis and/or Lyme arthritis weeks, months or even years later (2, 4).

A myriad of Lyme disease vaccine candidates in various stages of preclinical and clinical development are focused on a single *B. burgdorferi* antigen known as outer surface protein A (**OspA**) (5-14). OspA is a ~31 kDa lipoprotein expressed by *B. burgdorferi* during habitation of the tick midgut, then down regulated during transmission or upon entry into a vertebrate host (15). Decades ago, it was recognized that OspA vaccination or passive transfer of OspA antisera prevented *B. burgdorferi* infection in mouse and guinea pig models of tick-mediated transmission (16-20). Subsequent studies demonstrated that OspA antibodies inhibit one or more steps in spirochete migration from tick-to-mammal, although the exact mechanism(s) by which antibodies interrupt this process have not been fully elucidated (21-23). Nonetheless, recombinant OspA vaccines proved highly efficacious in Phase III clinical trials and one (LYMErix™) was licensed in the United States from 1998 to 2002 before being discontinued (14, 24, 25).

Despite ongoing investments in next-generation OspA vaccines, there remains a considerable gap in our understanding of the regions (epitopes) on OspA responsible for eliciting protective immunity to *B. burgdorferi* (26, 27). This was not necessarily an impediment with the first generation OspA vaccines like LYMErix™ because they were based on the single OspA

bioRxiv preprint doi: https://doi.org/10.1101/2024.01.23.576890; this version posted January 24, 2024. The copyright holder for this preprint (which was not certified by peer review) is the author/funder, who has granted bioRxiv a license to display the preprint in perpetuity. It is made available under aCC-BY-NC-ND 4.0 International license.

serotype (ST1) that predominates in the United States. Globally, however, there are at least seven OspA serotypes associated with Lyme disease-causing *B. burgdorferi* genospecies: *B. burgdorferi* (ST 1), *B. afzelii* (ST 2), *B. garinii* (ST 3, 5, 6, 7) and *B. bavariensis* (ST 4) (28, 29). Concerns about the lack of serotype cross protection has prompted the engineering of hexavalent and heptavalent vaccines consisting of recombinant full length and truncated OspA derivatives (10, 11, 30, 31). An alternative strategy would be to identify common or even conserved epitopes across the two or more of the OspA serotypes and use this information in the rational design of novel vaccine antigens (32). With this goal in mind, we recently generated an epitope map of OspA ST 1 using a collection of borreliacidal and transmission blocking human and mouse monoclonal antibodies (MAbs) revealing four distinct epitope bins or clusters (32, 33). Structural analysis of a subset of MAbs in complex with OspA ST1 has revealed detailed information about the nature of a select number of protective epitopes within these bins (26, 27, 34, 35).

Camelid-derived, single-domain antibodies, technically known as V_HHs, have emerged as tools to define the antigenic landscape of immunologically heterogeneous surface proteins, including notoriously polymorphic influenza virus hemagglutinin and the SARS-CoV-2 RBD (36-38). V_HHs derive from heavy chain-only antibodies (HCAbs) that exist with the Camelidae family, including llamas and alpacas (39). HCAbs consist of two heavy chains (homodimers) without light chain partners. The terminal V_H domain or V_HH confer antigen binding activity with properties and affinities not dissimilar to conventional IgG (40). V_HHs are small, stable and amenable to expression on the surface of bacteriophage M13 ("phage display"), thereby allowing antibody panning and affinity enrichment against targets of interest. In this report, we generated a phage-displayed V_HH library directed against OspA ST1 and identified 21 unique V_HHs within two epitope bins. Six of the monovalent V_HHs were expressed as human IgG1-Fc fusion proteins and been shown to have functional properties associated with protective human monoclonal antibodies, including *B. burgdorferi* agglutination, outer membrane damage, and complement-dependent borreliacidal activity. Finally, the V_HHs displayed unique reactivity profiles with the seven OspA serotypes associated with *B. burgdorferi* genospecies in the United States and Europe consistent with there being conserved epitopes across OspA serotypes that should be considered when designing and evaluating multivalent Lyme disease vaccines.

RESULTS

bioRxiv preprint doi: https://doi.org/10.1101/2024.01.23.576890; this version posted January 24, 2024. The copyright holder for this preprint (which was not certified by peer review) is the author/funder, who has granted bioRxiv a license to display the preprint in perpetuity. It is made available under aCC-BY-NC-ND 4.0 International license.

Isolation of distinct families of OspA-specific V_HHs. A phage-displayed V_HH library was constructed from two alpacas that had been immunized with recombinant OspA (rOspA) serotype 1 (ST1) from *B. burgdorferi* strain B31 in combination with the canine vaccine RECOMBITEK® Lyme, which contains lipidated OspA. The resulting phage library was subjected to 2 rounds of panning against rOspA, as described in the Materials and Methods. In total, 74 phages were isolated and subjected to DNA sequencing, revealing 21 unique clones (**Table 1**). Thirteen of the 21 clones were assigned to five different families based on complementarity determining region 3 (CDR3) sequence similarities. As an example, the alignment of the four members of the L8H8 family, along with the inferred germline V_H and J_H genes, is shown in **Figure S1**. The remaining 8 V_HHs were designated as "orphans" because they had no significant amino acid similarity to other V_HHs. Sequence analysis further suggests that 20 of 21 V_HHs likely derived from V_H 3-3 germline, with the exception (L8H7) derived from V_H 41 (41). From a structural standpoint, V_H 3-3-derived antibodies tend to have CDR3 elements that are pinned back towards the core of the antibody (42). The V_HHs were cloned into a pET32b-based vector and expressed as E-tagged thioredoxin fusion proteins in *E. coli* Rosetta Gami 2 cells. All 21 V_HHs bound to rOspA by ELISA with EC_{50} values that ranged from 1.8 nM to >1 μM (**Table 1**; **Figure 1**). V_HH dissociation constants (K_D) ranged from 0.28 to 457 nM, as determined by biolayer interferometry (**Table 1**; **Figure S2-S3**).

V_HHs cluster within two epitope bins on OspA. Four spatially distinct epitope bins (0-3) have been described along the length of OspA ST1 (33). Bin 0 constitutes a region of the N-terminus of OspA that is normally buried in the bacterial outer membrane and only accessible when OspA is released from the cell surface (26, 43). Bins 1 and 2 encompass OspA's central β-sheet (strands 8-13), while Bin 3 is situated within OspA's C-terminus (β-strands 16-21) and projects outward from the bacterial surface. MAbs capable of blocking *B. burgdorferi* tick to mouse transmission have been identified in bins 1, 2 and 3 (32, 33).

To epitope map the new panel of antibodies, V_HHs representative of the different clonal families were subjected to competitive BLI with MAbs from bin 1 (857-2), bin 2 (212-55), and bin 3 (LA-2) (**Figure S4**). Of the 11 representative V_HHs tested, four (L8H8, L8D3, L8H7, L8G12) were assigned to bin 1, based on competition with 857-2, and seven were assigned to bin 3, based on competition with LA-2 (**Table 1**; **Figure 2**). The seven V_HHs in bin 3 were subjected to further competition with MAbs 3-24 and 319-44, which recognize epitopes flanking LA-2.

bioRxiv preprint doi: https://doi.org/10.1101/2024.01.23.576890; this version posted January 24, 2024. The copyright holder for this preprint (which was not certified by peer review) is the author/funder, who has granted bioRxiv a license to display the preprint in perpetuity. It is made available under aCC-BY-NC-ND 4.0 International license.

Specifically, LA-2 targets the three exposed loops between β-strands 16-17, 18-19, and 20-21, as well as part of the C-terminal α-helix [**PDB ID** 1FJ1]. 3-24 targets β-strands 16-18, while 319-44 recognizes β-strands 19, 20, and 21, along with the loops between β-strands 16-17, 18-19, and 20-21 [**PDB ID** 7T25]. The seven V_HHs competed with 3-24, but not 319-44, thereby positioning their epitopes in proximity to β-strands 16-18 (pink shading; **Figure 2B**).

To better resolve antibody-OspA interactions within Bin 1, five V_HHs were subjected to epitope mapping by hydrogen exchange (HX)-mass spectrometry (MS) analysis using protocols optimized for OspA (33, 44). HX-MS is an increasingly powerful tool for epitope mapping in which the HX reaction is conducted in solution and captures antibody-induced changes in antigen backbone flexibility; strong reductions in HX are interpreted as points of antigen-antibody contact (45). As predicted, HX-MS indicated that all five V_HHs in bin 1 protected regions within OspA's central β-sheet (33). Specifically, L8H8 and two of its family members, L8A4 and L8D10, protected nearly identical OspA peptides corresponding to β-strands 10-14 (**Table 2**; **Figure 3**). The "orphan" V_HH, L8G12, also protected β-strands 11-14, while L8D3 (a member of the L8A10 family) protected β-strands 11-13 (**Table 2**; **Figure 3**). These results demonstrate that β-strands 10-14 constitute a V_HH "hotspot" within bin 1.

Functional activity associated with OspA-specific monovalent V_HHs and bivalent V_HH-IgG constructs. A hallmark of OspA antibodies, and certain monovalent Fabs, is their capacity to induce agglutination of *B. burgdorferi* in culture (46-48). We have postulated that agglutination explains, at least in part, how OspA antibodies entrap *B. burgdorferi* within the tick midgut and block transmission to vertebrate hosts (46). We employed a quantitative flow cytometry-based assay to examine whether any of the 21 monovalent OspA V_HHs induced agglutination of live *B. burgdorferi* B31 (46). The handful of V_HHs with dissociation constants $\geq$1000 nM did not promote spirochete agglutination (**Table 1**). The remaining V_HHs displayed a range of agglutinating activities, although with no clear relationship between agglutination and epitope specificity (i.e., bin 1 or bin 3) or agglutination and OspA binding affinity (K_D). For example, L8D9 (bin 3) and L8G12 (bin 1) each have sub-nanomolar binding affinities for OspA, but neither induced notable agglutination of *B. burgdorferi* (**Table 1**). L8D3 (bin 1) and L8C3 (bin 3) have comparable affinities for OspA (10.4 vs 8.82 nM), but L8D3 is a poor agglutinator while L8C3 was a good agglutinator (0.28% vs 12.5%).

bioRxiv preprint doi: https://doi.org/10.1101/2024.01.23.576890; this version posted January 24, 2024. The copyright holder for this preprint (which was not certified by peer review) is the author/funder, who has granted bioRxiv a license to display the preprint in perpetuity. It is made available under aCC-BY-NC-ND 4.0 International license.

To investigate the impact of antibody avidity on spirochete agglutination, three V_HHs each from bin 1 and bin 3 were grafted onto human IgG1 Fc elements and expressed as bivalent molecules in Expi293 cells (49). The six V_HH-IgG fusion proteins recognized native OspA on the surface of live *B. burgdorferi* B31 to levels similar to LA-2, as demonstrated by flow cytometry (**Table 3**; **Figure 4**). The V_HH-IgGs also had *B. burgdorferi* agglutinating activities that were significantly greater than their monovalent V_HH counterparts (**Table 4**). For example, V_HH L8D3 (bin 1) had <1% agglutinating activity as a monomer but >17% activity as a V_HH-IgG Fc fusion protein (**Table 3**; **Figure 4**). L8G12 (bin 1) and L8D9 (bin 3) also demonstrated >10-fold increase in agglutinating activity when expressed as an IgG fusion protein. In all instances, antibody-mediated spirochete agglutination correlated with a corresponding increase in *B. burgdorferi* outer membrane permeability, as reflected by elevated levels of propidium iodine (PI) uptake (**Table 3; Figure 4**).

The ability of OspA antibodies to elicit borreliacidal activity is considered a correlate of protection in Lyme disease (50). Therefore, we next assessed the OspA-specific V_HHs and V_HH-IgG Fc fusion proteins for the ability to promote complement-mediated killing of a fluorescent *B. burgdorferi* B31 reporter strain (33). As expected, none of the monovalent V_HHs were borreliacidal (**data not shown**). However, all six V_HH-IgG Fc fusion proteins were borreliacidal. The three bin 1 V_HH-IgGs (L8D3, L8G12, L8H8) were tested side-by-side with 857-2, while the three bin 3 V_HH-IgGs (L8A9, L8C3, L8D9) were compared to LA-2. The six V_HH-IgGs tested had EC_{50} values between 1.25 and 2.5 nM (**Table 3**; **Figure 5**). By comparison, 857-2 and LA-2 had EC_{50} values of 1.25 and ~0.75 nM, respectively (**Figure 5**). Collectively, these results demonstrate the ability of alpaca-derived V_HHs to recognize native OspA on the surface of live *B. burgdorferi* and promote spirochete agglutination, outer membrane damage, and complement-mediated borreliacidal activity.

Cross-reactivity of V_HHs with OspA serotypes ST1-7 reveal additional levels of epitope diversity. There are seven OspA serotypes (ST1-7) within *B. burgdorferi sensu latu* strains associated with disease (**Figure 6A**) (14, 29). The serotypes were originally defined based on reactivity profiles with a panel of OspA MAbs. LA-2 (bin 3), for example, recognizes OspA ST1 but not ST 2-7, while 857-2 (bin 1) is predicted to react with all 7 serotypes (32). To assess the specificity of the alpaca-derived V_HHs, the three bin 1 V_HH-IgGs (L8D3, L8G12, L8H8) and three bin 3 V_HH-IgGs (L8A9, L8C3, L8D9) were evaluated in an OspA ST 1-7

bioRxiv preprint doi: https://doi.org/10.1101/2024.01.23.576890; this version posted January 24, 2024. The copyright holder for this preprint (which was not certified by peer review) is the author/funder, who has granted bioRxiv a license to display the preprint in perpetuity. It is made available under aCC-BY-NC-ND 4.0 International license.

indirect ELISA (**Figure 6B**). As predicted, 857-2 reacted with all seven OspA serotypes, while LA-2 reacted with only ST-1. The V_HHs displayed unique reactivity patterns relative to 857-2 and LA-2. Within bin 1, for example, L8D3 recognized ST1 exclusively, while L8G12 and L8H8 recognized ST 1, 2, 4 and 5. Within bin 3, L8D9 reacted exclusively with serotype 1 (like LA-2), but L8A9 and L8C3 recognized ST1 plus serotype 6 (L8A9) or serotype 4 (L8C3). These results reveal a greater degree of B cell epitope diversity on OspA than previously recognized and have important implications for multivalent vaccine design.

DISCUSSION

Single-domain antibodies (V_HHs) have emerged as invaluable tools and reagents in the development of next-generation diagnostics, therapeutics, and vaccines for a range of infectious diseases (40). With this in mind, we sought to generate a diverse collection of V_HHs against the Lyme disease vaccine antigen, OspA, as a means to better define the conserved and variable epitopes on the different OspA serotypes associated with borreliacidal activity. We constructed an immune V_HH-phage display library from two OspA immunized alpacas and subjected the library to rounds of affinity enrichment on recombinant OspA serotype 1 (ST1). The screen yielded 21 unique OspA-specific V_HHs with a range of binding affinities, epitope specificities, serotype reactivities, and functional activities *in vitro*. A subset of V_HHs were expressed as human IgG1-Fc fusion proteins and shown to promote complement-independent *B. burgdorferi* agglutination, as well as complement-dependent borreliacidal activity. In addition to expanding our understanding of functional B cell epitopes on OspA, we expect that this unique collection of V_HHs will have applications for pre-clinical and clinical Lyme disease vaccine development.

The 21 V_HHs described in this study have epitope reactivity profiles that are both similar and different from previously reported OspA-specific mouse and human MAbs (17, 19, 26-29, 33, 34, 43, 51). On the one hand, the V_HHs fell within two previously described epitope bins based on competition with human MAb 857-2 (bin 1) and mouse MAb LA-2 (bin 3). On the other hand, the V_HHs displayed unique reactivity profiles within those respective bins. For example, within bin 1, 857-2 recognized all seven OspA serotypes, while L8G12 and L8H8 were reactive with serotypes 1, 2, 4 and 5; L8D3 was only reactive with serotype 1. This result is consistent with pioneering work by Wilske and colleagues demonstrating that there are

bioRxiv preprint doi: https://doi.org/10.1101/2024.01.23.576890; this version posted January 24, 2024. The copyright holder for this preprint (which was not certified by peer review) is the author/funder, who has granted bioRxiv a license to display the preprint in perpetuity. It is made available under aCC-BY-NC-ND 4.0 International license.

conserved, partially conserved, and serotype-specific epitopes within OspA's central β-sheet (strand 8-14) (29).

Competition assays with three different bin 3 MAbs (LA-2, 319-44, 3-24) enabled us to localize epitopes recognized by seven different V_HHs to OspA β-strands 16-18 (residues 195-227). However, even within this relatively restricted region of OspA, there was notable epitope diversity, as exemplified by differential serotype reactivities of L8A9 and L8C3 as compared to LA-2. Specifically, LA-2 recognized serotype 1 exclusively, while L8A9 and L8C3 were reactive with serotypes 1, 4, and 6. This observation challenges the notion that the C-terminal region of OspA elicits only serotype-specific antibody responses (28, 52).

From the standpoint of V_HH clonal diversity, we identified five distinct antibody families that collectively accounted for more than half the 21 V_HHs. The L8H8 family is notable for having the most members (four) recovered in our current screening protocol, as well as the V_HH with the highest affinity for OspA (L8H8; 0.28 nM). As expected, the three L8H8 family members we subjected to epitope mapping by HX-MS had virtually identical protection profiles. However, within the family, the dissociation constants ranged by at least an order of magnitude from 0.28 nM (L8H8) to >2 nM (L8E1), likely due to variations in CDR1 and CDR2 interactions with OspA. This novel collection of antibodies with identical epitope specificities but varying binding affinities can be used as a toolkit to investigate the open question of the relative contribution of binding affinity in OspA antibody effector function. As a case in point, studies are planned to evaluate the L8H8 family of V_HHs as well as V_HH-IgGs for the ability to block transmission of *B. burgdorferi* in a mouse model of tick-mediated infection, with the expectation that there will be a direct relationship between binding affinity and protection. Indeed, as shown in Table 1, the contribution of binding affinity on the ability of the L8H8 family of V_HHs to promote spirochete agglutination is already somewhat evident.

While the V_HHs and V_HH-IgGs described in this study have yet to be tested for *B. burgdorferi* transmission blocking activity in a mouse model, we would predict, based on *in vitro* activities, that at least a subset will be effective *in vivo*. Most significant in our minds was the observation that a subset of monovalent V_HHs and all six bivalent V_HH-IgGs could promote spirochete agglutination and induce alterations in outer membrane permeability. We have argued that such activities, should they occur in the context of the tick midgut, would impair the ability of spirochetes to migrate across the midgut epithelium and onto the salivary glands (46). The

bioRxiv preprint doi: https://doi.org/10.1101/2024.01.23.576890; this version posted January 24, 2024. The copyright holder for this preprint (which was not certified by peer review) is the author/funder, who has granted bioRxiv a license to display the preprint in perpetuity. It is made available under aCC-BY-NC-ND 4.0 International license.

V_HH-IgGs (but not the monovalent V_HHs themselves) were also extremely effective at promoting complement-mediated killing of B. *burgdorferi*. While the role of complement-mediated killing in transmission inhibition within the tick remains an open question, OspA antibody-mediated complement-dependent killing *in vitro* does correlate with protection *in vivo* (50). Thus, we predict that the six V_HH-IgGs described in Table 3 will likely prove effective *in vivo*.

We envision at least two potential applications of the V_HHs to Lyme disease vaccine development. First is their use in "equivalency" assays. For example, in the pivotal clinical trial associated with the LYMErix vaccine, a competitive ELISA with LA-2 was used as a surrogate measure of protective antibody titers limited to OspA serotype 1 (24). Similar, albeit more sophisticated, competition assays using a panel of V_HHs directed against known protective epitopes on OspA serotypes 1-7 could be employed for the evaluation of future multivalent Lyme disease vaccines. Second, the OspA V_HHs could be employed in identity testing, epitope integrity analysis, and release assays associated with vaccine manufacturing and mandated by regulatory agencies. Identity testing will be especially relevant when evaluating recombinant or nucleic acid-based hexavalent and even heptavalent Lyme disease vaccines (6). We have also described other antibody-based applications for vaccine development that may be pertinent to Lyme disease (53).

Materials and Methods

Alpaca immunization and V_HH phage display library preparation. Two alpacas (*Vicugna pacos*) were immunized four times, each about three weeks apart, with various combinations of recombinant OspA serotype 1 from *B. burgdorferi* strain B31 [UniProt P0CL66] and the veterinary vaccine RECOMBITEK® Lyme (Boehringer Ingelheim). The first immunization consisted of a full dose of RECOMBITEK® only. The next vaccination the alpacas received a half dose of RECOMBITEK® and 200 µg of rOspA. The final two vaccinations consisted of a half dose of RECOMBITEK® and 100 µg of rOspA. Following the final immunization, both animals had OspA antibody endpoint titers > 500,000. Five days following the final immunization, lymphocytes were isolated from whole blood and used to generate a V_HH M13 phage-display library, as described (54, 55). The library passed all QC testing and was estimated to contain ~1.3 x 10^7 independent clones.

bioRxiv preprint doi: https://doi.org/10.1101/2024.01.23.576890; this version posted January 24, 2024. The copyright holder for this preprint (which was not certified by peer review) is the author/funder, who has granted bioRxiv a license to display the preprint in perpetuity. It is made available under aCC-BY-NC-ND 4.0 International license.

Recombinant OspA. Recombinant OspA (non-lipidated) ST1 from B31 [NCBI reference WP_010890378.1] was expressed in *E.coli* and purified as described (33, 34). Purified, recombinant OspA serotypes 2-7 were kindly provided by Dr. Meredith Finn (Moderna, Inc).

V_HH Identification and Expression. The V_HH M13 phage-display library was subjected to two rounds of affinity enrichment (panning) against immobilized recombinant OspA on Nunc-Immunotubes™ (Thermo Fisher Scientific, Waltham, MA) using protocols described elsewhere (56). The first panning was low stringency (10 ug/mL coat), after which phages were eluted with glycine HCl [pH 2.2] and then amplified in *E. coli*. The phages were then subjected to a second round of screening at high stringency (1 ug/mL coat). After the second round of panning, 95 clones were chosen at random and grown overnight at 37° C in a 96 well plate. Replica cultures in 96 well plates were grown to log phase, then induced overnight with IPTG (3 mM). Resulting supernatants were assayed by ELISA for reactivity with rOspA. 74 clones were found to bind to OspA, and all were then DNA sequenced. 21 V_HHs, belonging to 12 different sequence families, were found to be sufficiently unique to characterize further. The DNA coding region for these V_HHs was restriction digested out of the phagemid vector and inserted into a pET-32b vector for expression as a recombinant thioredoxin fusion protein containing a His-Tag in the linker region, and an E-tag for detection at the C-terminus. V_HHs were transformed into and expressed in Rosetta Gami 2 (DE3) pLacI competent *E. coli* (Millipore Sigma), induced with IPTG (1 mM), and purified in a nickel column. Concentration was determined by OD_{280} and the recombinant protein extinction coefficient.

ELISA. OspA was coated overnight in 96-well immunoplates at 1 ug/mL in 100 uL of PBS. The following morning, the wells were blocked for 2 hours with 2% goat serum in PBS with 0.1% Tween 20 (PBST). During blocking, V_HHs were 5-fold diluted in PBS in a separate 96-well non-binding plate, starting at 10 uM. The V_HHs were then applied to the OspA coated plate for 1 hour and allowed to bind. After washing the wells with PBST, HRP-conjugated anti-E-tag secondary antibody (Bethyl Labs, Waltham MA) was added to the well for 1 hour to detect bound V_HHs. After a final wash with PBST, 100 uL SureBlue TMB (SeraCare) was added to the wells for about 10 minutes to visualize binding. The colorometric reaction was quenched with 1M

bioRxiv preprint doi: https://doi.org/10.1101/2024.01.23.576890; this version posted January 24, 2024. The copyright holder for this preprint (which was not certified by peer review) is the author/funder, who has granted bioRxiv a license to display the preprint in perpetuity. It is made available under aCC-BY-NC-ND 4.0 International license.

phosphoric acid, and absorbance at 450 nm was measured on a SpectraMax iD3 plate reader (Molecular Biosystems) using SoftMax Pro version 7.1 software.

Biolayer Interferometry (BLI). BLI experiments were carried out using an Octet RED96e Biolayer Interferometer (Sartorius AG, Gottingen, Germany) using the Data Acquisition 12.0 software. Raw sensor data was loaded into the Data Analysis HT 12.0 software for analysis. Biotinylated OspA (5 µg/mL) in PBS containing 2% w/v BSA was captured onto streptavidin biosensors (#18-5019, Sartorius) for 5 min. After 5 minutes of baseline in buffer, sensors were then exposed to a 2-fold dilution series of V_HH, ranging from 200 to 3.125 nM, for 5 minutes to allow association. The sensors were then immediately dipped into wells containing buffer alone for 30 minutes to allow dissociation of the V_HH. An eighth sensor was also loaded with Biotinylated OspA, but was not exposed to V_HHs, and was thus used as a background drift control, and subtracted from the other sensor data. After each V_HH, the OspA-coated sensors were completely regenerated by a 30 second cycle consisting of three repeats of 5 sec in 0.2 M glycine (pH 2.2) and 5 sec in buffer. Sensor data was fit to a 1:1 binding model.

For competition experiments biotinylated OspA (5 µg/mL) in buffer was captured onto streptavidin biosensors for 5 minutes. After 3 minutes of baseline in buffer, sensors were then exposed to a primary mAb at a concentration of 15 µg/mL in buffer for 10 minutes to permit the association signal to saturate. The sensors were then immediately dipped into wells containing competitor V_HH (1 uM) for 10 min. After each primary-secondary pairing, the sensors were regenerated by a 30 second cycle consisting of three repeats of 5 sec in 0.2 M glycine (pH 2.2) and 5 sec in buffer. The total binding signal (in nm) obtained for the secondary V_HH, from the end of the primary mAb, was then recorded for each specific primary-secondary pair. The data for each V_HH was normalized to the binding signal for that V_HH vs mAb 212-55, which no V_HH competed with, then plotted as a heat map using GraphPad Prism 9.

HX-MS. Differential hydrogen exchange-mass spectrometry (HX-MS) was used to identify regions of OspA exhibiting altered amide hydrogen exchange kinetics in the presence of an excess of each V_HH using methods fully described previously (33, 44). In brief, OspA alone or in the presence of molar excess V_HH was diluted ten-fold with 20 mM phosphate, 100 mM NaCl,

bioRxiv preprint doi: https://doi.org/10.1101/2024.01.23.576890; this version posted January 24, 2024. The copyright holder for this preprint (which was not certified by peer review) is the author/funder, who has granted bioRxiv a license to display the preprint in perpetuity. It is made available under aCC-BY-NC-ND 4.0 International license.

pH 7.40 buffer containing deuterium oxide. After various intervals of exchange ranging between 20 s and 24 hr, the exchange reaction was rapidly quenched by acidification. HX-MS measurements were completed either in triplicate at five exchange times (referred to as "complete") or single measurements at three exchange times (referred to as "screening"). The quenched samples were rapidly digested with pepsin to yield deuterium-labeled OspA peptides. The deuterium incorporation was measured by LC-MS. Differences in hydrogen exchange were quantified as the mean exchange by bound OspA minus mean exchange by free OspA. Since peptides of different lengths contain different numbers of amide hydrogens, the results were normalized based on the amount of deuteration in maximally deuterated control samples. The resulting quantity, $\Delta\overline{HX}$, represents this mean fractional difference; negative values indicate slower hydrogen exchange by bound OspA.

Surface binding, membrane integrity, and agglutination analysis of *B. burgdorferi*. *B. burgdorferi* strain B31 (ATCC) was cultured in BSK-II media (minus gelatin) at 33°C with 2.5% CO_2 (57). Cultures at mid-log phase were diluted 1/10 in medium and grown at 23°C to early-log phase to induce high levels of OspA expression (46). Bacteria were collected by centrifugation (3,300 x *g*), washed with PBS, resuspended in BSK II medium (minus phenol red), and allowed to recover at room temperature for 30 min. A total of $5x10^6$ cells in 50 µl were incubated with an OspA-specific VHH or VHH-IgG Fc at a final concentration of 10 µg/ml at 37 °C for 1 h. Incubation with 10 µg/ml of an unrelated ricin-specific VHH (V8B3) or IgG (PB10) were included as negative controls, while chimeric LA-2 IgG1 was run as a positive control (33). Reaction volumes were increased with the addition of 450 µl of BSK II medium (minus phenol red) and incubated at 37°C for 30 min with either a 1/500 dilution of PE-labeled anti-6xHis tag mouse MAb (Biolegend, San Diego, CA) to detect VHHs or Alexa Fluor 647-labeled goat anti-human IgG (H+L) (Invitrogen) to detect VHH-IgG Fcs. All mixtures were transferred into a 5 mL round bottom polystyrene test tube (Corning) with 250 µl of PBS. For VHH-IgG Fc reactions, 0.75 µM propidium iodide (PI) (Sigma-Aldrich) was added immediately before analysis to measure membrane integrity. All samples were analyzed on a BD FACSCalibur flow cytometer (BD Biosciences). Bacteria were gated on forward scatter (FSC) and side scatter (SSC) to assess aggregate size and granularity, and 20,000 events were counted. Alexa Fluor 647 labeling (FL4), PE labeling (FL3) or PI staining (FL3), and agglutination (FSC/SSC) were

bioRxiv preprint doi: https://doi.org/10.1101/2024.01.23.576890; this version posted January 24, 2024. The copyright holder for this preprint (which was not certified by peer review) is the author/funder, who has granted bioRxiv a license to display the preprint in perpetuity. It is made available under aCC-BY-NC-ND 4.0 International license.

390 measured using CellQuest Pro (BD Biosciences). Agglutination was calculated as the sum of
391 events in the upper-left, upper-right, and lower-right quadrants relative to total events (46).
392
393 **Borreliacidal assays.** V_HH-IgG Fcs were assessed for complement-dependent borreliacidal
394 activity via fluorescence-based serum bactericidal assay essentially as described (33). Slight
395 modifications to the previous assay include the mCherry open reading frame (ORF) within the
396 reporter plasmid (pGW163) was replaced with a codon-optimized variant of mScarlet-I
397 engineered for efficient expression in *Borrelia* species (G. Willsey, N. Mantis, *manuscript in*
398 *preparation*). The resulting plasmid, pGW189, was subsequently transformed into *B. burgdorferi*
399 B31-5A4 following established protocols (58). The resulting IPTG-inducible mScarlet-I viability
400 reporter strain was designated GGW979.
401 For each assay, glycerol stocks of GGW979 were thawed at RT and transferred to sterile 50 ml
402 centrifuge tubes containing 45 ml of BSK-II medium supplemented with 40 µg/ml of
403 gentamicin. The cultures were then incubated at 33°C without agitation for three days. On the
404 day of the assay, spirochetes were collected via centrifugation, the culture media was removed,
405 and the cells were then resuspended at 3 x10^7 spirochetes per ml in phenol-free BSKII medium
406 supplemented with gentamicin (40 µg/mL) and 20 % human complement sera (SigmaAldrich).
407 The spirochetes were then mixed 1:1 v/v with serial dilutions of each V_HH-Fc IgG1 antibody that
408 had been prepared in phenol-free BSKII supplemented with gentamicin (40 µg/mL) and 20 %
409 human complement. Following sample addition, each reaction contained and 5x10^6 spirochetes
410 per well and 40 nM and 0.325 nM of each antibody. 857-2 and LA-2 IgG1 MAbs were included
411 in each assay to serve as positive controls (33). Untreated/non-induced and untreated/IPTG-
412 induced controls were similarly included to determine baseline and peak fluorescence.
413
414 Following sample addition, assay plates were incubated overnight at 37 °C with 5 % CO2. After
415 18-20 h, 1 mM IPTG was added to each well (minus the untreated control) to induce expression
416 of the fluorescent reporter in surviving spirochetes. Assay plates were then returned to the
417 incubator. Forty-eight hours later, Median Fluorescence Intensity (MFI) was recorded three
418 times per plate at 569 nm (Ex)/611 nm (Em) using a SpectraMax iD3 microplate reader
419 (Molecular Biosystems) and SoftMax Pro version 7.1 software. The resulting values were
420 averaged, and the data was then normalized using the untreated (-IPTG) and untreated (+IPTG)

bioRxiv preprint doi: https://doi.org/10.1101/2024.01.23.576890; this version posted January 24, 2024. The copyright holder for this preprint (which was not certified by peer review) is the author/funder, who has granted bioRxiv a license to display the preprint in perpetuity. It is made available under aCC-BY-NC-ND 4.0 International license.

controls to set baseline (0) and peak (100) MFI. Following normalization, the data was analyzed using GraphPad Prism Version 9.0. Data reported encompasses three separate experiments, with EC_{50} values determined by the lowest dilution of antibody resulting in 50% reduction in MFI relative to normalized controls.

Author Contributions

DJV screened the V_HH phage display library, sequenced the V_HHs, conducted Octet and ST1-7 ELISA experiments, and wrote and edited the manuscript; SB cloned and expressed VHHs in *E.coli*, and performed OspA ELISA experiments; CLP conducted *B. burgdorferi* flow cytometry experiments; GGW conducted *B. burgdorferi* borreliacidal assays; JMT and CBS constructed the V_HH phage display library; HMEH and DDW conducted HX-MS and data analysis; MJR expressed and purified all recombinant proteins; LC expressed and purified the VHH-Fc antibodies; NJM was responsible for project leadership, funding acquisition, and writing the manuscript.

ACKNOWLEDGEMENTS

The authors gratefully acknowledge Elizabeth Cavosie (Wadsworth Center) for administrative assistance and grants management. We thank the Wadsworth Center's Immunology Core for flow cytometry assistance and the Cell culture and media core for BSK II medium. We extend our special thanks to Drs. Meredith Finn and Chris Dold (Moderna, Inc, Cambridge, MA) for providing recombinant OspA serotypes 1-7. This work was supported by the National Institute of Allergy and Infectious Disease (NIAID), National Institutes of Health, Department of Health and Human Services, Contract No. 75N93019C00040 (PI/PD Mantis).

REFERENCES

1. Kugeler KJ, Schwartz AM, Delorey MJ, Mead PS, Hinckley AF. 2021. Estimating the Frequency of Lyme Disease Diagnoses, United States, 2010-2018. Emerg Infect Dis 27:616-619.
2. Bobe JR, Jutras BL, Horn EJ, Embers ME, Bailey A, Moritz RL, Zhang Y, Soloski MJ, Ostfeld RS, Marconi RT, Aucott J, Ma'ayan A, Keesing F, Lewis K, Ben Mamoun C, Rebman AW, McClune ME, Breitschwerdt EB, Reddy PJ, Maggi R, Yang F, Nemser B, Ozcan A, Garner O, Di Carlo D, Ballard Z, Joung HA, Garcia-Romeu A, Griffiths RR,

bioRxiv preprint doi: https://doi.org/10.1101/2024.01.23.576890; this version posted January 24, 2024. The copyright holder for this preprint (which was not certified by peer review) is the author/funder, who has granted bioRxiv a license to display the preprint in perpetuity. It is made available under aCC-BY-NC-ND 4.0 International license.

Baumgarth N, Fallon BA. 2021. Recent Progress in Lyme Disease and Remaining Challenges. Front Med (Lausanne) 8:666554.

3. Steere AC, Strle F, Wormser GP, Hu LT, Branda JA, Hovius JW, Li X, Mead PS. 2016. Lyme borreliosis. Nat Rev Dis Primers 2:16090.

4. Lochhead RB, Strle K, Arvikar SL, Weis JJ, Steere AC. 2021. Lyme arthritis: linking infection, inflammation and autoimmunity. Nat Rev Rheumatol 17:449-461.

5. Pine M, Arora G, Hart TM, Bettini E, Gaudette BT, Muramatsu H, Tombacz I, Kambayashi T, Tam YK, Brisson D, Allman D, Locci M, Weissman D, Fikrig E, Pardi N. 2023. Development of an mRNA-lipid nanoparticle vaccine against Lyme disease. Mol Ther 31:2702-2714.

6. Bezay N, Hochreiter R, Kadlecek V, Wressnigg N, Larcher-Senn J, Klingler A, Dubischar K, Eder-Lingelbach S, Leroux-Roels I, Leroux-Roels G, Bender W. 2023. Safety and immunogenicity of a novel multivalent OspA-based vaccine candidate against Lyme borreliosis: a randomised, phase 1 study in healthy adults. Lancet Infect Dis 23:1186-1196.

7. Federizon J, Lin YP, Lovell JF. 2019. Antigen Engineering Approaches for Lyme Disease Vaccines. Bioconjug Chem 30:1259-1272.

8. Federizon J, Frye A, Huang WC, Hart TM, He X, Beltran C, Marcinkiewicz AL, Mainprize IL, Wills MKB, Lin YP, Lovell JF. 2020. Immunogenicity of the Lyme disease antigen OspA, particleized by cobalt porphyrin-phospholipid liposomes. Vaccine 38:942-950.

9. Klouwens MJ, Salverda MLM, Trentelman JJ, Ersoz JI, Wagemakers A, Gerritzen MJH, van der Ley PA, Hovius JW. 2021. Vaccination with meningococcal outer membrane vesicles carrying Borrelia OspA protects against experimental Lyme borreliosis. Vaccine 39:2561-2567.

10. Kamp HD, Swanson KA, Wei RR, Dhal PK, Dharanipragada R, Kern A, Sharma B, Sima R, Hajdusek O, Hu LT, Wei CJ, Nabel GJ. 2020. Design of a broadly reactive Lyme disease vaccine. NPJ Vaccines 5:33.

11. Comstedt P, Schüler W, Meinke A, Lundberg U. 2017. The novel Lyme borreliosis vaccine VLA15 shows broad protection against Borrelia species expressing six different OspA serotypes. PLoS One 12:e0184357.

12. Dattwyler RJ, Gomes-Solecki M. 2022. The year that shaped the outcome of the OspA vaccine for human Lyme disease. NPJ Vaccines 7:10.

13. O'Bier NS, Hatke AL, Camire AC, Marconi RT. 2021. Human and Veterinary Vaccines for Lyme Disease. Curr Issues Mol Biol 42:191-222.

14. Wormser GP. 2022. A brief history of OspA vaccines including their impact on diagnostic testing for Lyme disease. Diagn Microbiol Infect Dis 102:115572.

15. Srivastava SY, de Silva AM. 2008. Reciprocal expression of ospA and ospC in single cells of Borrelia burgdorferi. J Bacteriol 190:3429-33.

16. Fikrig E, Barthold SW, Kantor FS, Flavell RA. 1990. Protection of mice against the Lyme disease agent by immunizing with recombinant OspA. Science 250:553-6.

17. Schaible UE, Kramer MD, Eichmann K, Modolell M, Museteanu C, Simon MM. 1990. Monoclonal antibodies specific for the outer surface protein A (OspA) of Borrelia burgdorferi prevent Lyme borreliosis in severe combined immunodeficiency (scid) mice. Proc Natl Acad Sci U S A 87:3768-72.

bioRxiv preprint doi: https://doi.org/10.1101/2024.01.23.576890; this version posted January 24, 2024. The copyright holder for this preprint (which was not certified by peer review) is the author/funder, who has granted bioRxiv a license to display the preprint in perpetuity. It is made available under aCC-BY-NC-ND 4.0 International license.

18. Simon MM, Schaible UE, Kramer MD, Eckerskorn C, Museteanu C, Müller-Hermelink HK, Wallich R. 1991. Recombinant outer surface protein a from Borrelia burgdorferi induces antibodies protective against spirochetal infection in mice. J Infect Dis 164:123-32.
19. Bockenstedt LK, Fikrig E, Barthold SW, Kantor FS, Flavell RA. 1993. Inability of truncated recombinant Osp A proteins to elicit protective immunity to Borrelia burgdorferi in mice. J Immunol 151:900-6.
20. de Silva AM, Telford SR, 3rd, Brunet LR, Barthold SW, Fikrig E. 1996. Borrelia burgdorferi OspA is an arthropod-specific transmission-blocking Lyme disease vaccine. J Exp Med 183:271-5.
21. Fikrig E, Telford SR, 3rd, Barthold SW, Kantor FS, Spielman A, Flavell RA. 1992. Elimination of Borrelia burgdorferi from vector ticks feeding on OspA-immunized mice. Proc Natl Acad Sci U S A 89:5418-21.
22. de Silva AM, Fish D, Burkot TR, Zhang Y, Fikrig E. 1997. OspA antibodies inhibit the acquisition of Borrelia burgdorferi by Ixodes ticks. Infect Immun 65:3146-50.
23. Rathinavelu S, Broadwater A, de Silva AM. 2003. Does host complement kill Borrelia burgdorferi within ticks? Infect Immun 71:822-9.
24. Steere AC, Sikand VK, Meurice F, Parenti DL, Fikrig E, Schoen RT, Nowakowski J, Schmid CH, Laukamp S, Buscarino C, Krause DS. 1998. Vaccination against Lyme disease with recombinant Borrelia burgdorferi outer-surface lipoprotein A with adjuvant. Lyme Disease Vaccine Study Group. N Engl J Med 339:209-15.
25. Sigal LH, Zahradnik JM, Lavin P, Patella SJ, Bryant G, Haselby R, Hilton E, Kunkel M, Adler-Klein D, Doherty T, Evans J, Molloy PJ, Seidner AL, Sabetta JR, Simon HJ, Klempner MS, Mays J, Marks D, Malawista SE. 1998. A vaccine consisting of recombinant Borrelia burgdorferi outer-surface protein A to prevent Lyme disease. Recombinant Outer-Surface Protein A Lyme Disease Vaccine Study Consortium. N Engl J Med 339:216-22.
26. Li H, Dunn JJ, Luft BJ, Lawson CL. 1997. Crystal structure of Lyme disease antigen outer surface protein A complexed with an Fab. Proc Natl Acad Sci U S A 94:3584-9.
27. Ding W, Huang X, Yang X, Dunn JJ, Luft BJ, Koide S, Lawson CL. 2000. Structural identification of a key protective B-cell epitope in Lyme disease antigen OspA. J Mol Biol 302:1153-64.
28. Wilske B, Luft B, Schubach WH, Zumstein G, Jauris S, Preac-Mursic V, Kramer MD. 1992. Molecular analysis of the outer surface protein A (OspA) of Borrelia burgdorferi for conserved and variable antibody binding domains. Med Microbiol Immunol 181:191-207.
29. Wilske B, Preac-Mursic V, Gobel UB, Graf B, Jauris S, Soutschek E, Schwab E, Zumstein G. 1993. An OspA serotyping system for Borrelia burgdorferi based on reactivity with monoclonal antibodies and OspA sequence analysis. J Clin Microbiol 31:340-50.
30. Comstedt P, Hanner M, Schuler W, Meinke A, Lundberg U. 2014. Design and development of a novel vaccine for protection against Lyme borreliosis. PLoS One 9:e113294.
31. Comstedt P, Hanner M, Schuler W, Meinke A, Schlegl R, Lundberg U. 2015. Characterization and optimization of a novel vaccine for protection against Lyme borreliosis. Vaccine 33:5982-8.

bioRxiv preprint doi: https://doi.org/10.1101/2024.01.23.576890; this version posted January 24, 2024. The copyright holder for this preprint (which was not certified by peer review) is the author/funder, who has granted bioRxiv a license to display the preprint in perpetuity. It is made available under aCC-BY-NC-ND 4.0 International license.

32. Wang Y, Kern A, Boatright NK, Schiller ZA, Sadowski A, Ejemel M, Souders CA, Reimann KA, Hu L, Thomas WD, Jr., Klempner MS. 2016. Pre-exposure Prophylaxis With OspA-Specific Human Monoclonal Antibodies Protects Mice Against Tick Transmission of Lyme Disease Spirochetes. J Infect Dis 214:205-11.
33. Haque HME, Ejemel M, Vance DJ, Willsey G, Rudolph MJ, Cavacini LA, Wang Y, Mantis NJ, Weis DD. 2022. Human B Cell Epitope Map of the Lyme Disease Vaccine Antigen, OspA. ACS Infect Dis doi:10.1021/acsinfecdis.2c00346.
34. Schiller ZA, Rudolph MJ, Toomey JR, Ejemel M, LaRochelle A, Davis SA, Lambert HS, Kern A, Tardo AC, Souders CA, Peterson E, Cannon RD, Ganesa C, Fazio F, Mantis NJ, Cavacini LA, Sullivan-Bolyai J, Hu LT, Embers ME, Klempner MS, Wang Y. 2021. Blocking Borrelia burgdorferi transmission from infected ticks to nonhuman primates with a human monoclonal antibody. J Clin Invest 131.
35. Rudolph MJ, Davis SA, Haque HME, Ejemel M, Cavacini LA, Vance DJ, Willsey GG, Piazza CL, Weis DD, Wang Y, Mantis NJ. 2023. Structure of a transmission blocking antibody in complex with Outer surface protein A from the Lyme disease spirochete, Borreliella burgdorferi. Proteins doi:10.1002/prot.26549.
36. Laursen NS, Friesen RHE, Zhu X, Jongeneelen M, Blokland S, Vermond J, van Eijgen A, Tang C, van Diepen H, Obmolova G, van der Neut Kolfschoten M, Zuijdgeest D, Straetemans R, Hoffman RMB, Nieusma T, Pallesen J, Turner HL, Bernard SM, Ward AB, Luo J, Poon LLM, Tretiakova AP, Wilson JM, Limberis MP, Vogels R, Brandenburg B, Kolkman JA, Wilson IA. 2018. Universal protection against influenza infection by a multidomain antibody to influenza hemagglutinin. Science 362:598-602.
37. Czajka TF, Vance DJ, Mantis NJ. 2021. Slaying SARS-CoV-2 One (Single-domain) Antibody at a Time. Trends Microbiol 29:195-203.
38. Jiang J, Boughter CT, Ahmad J, Natarajan K, Boyd LF, Meier-Schellersheim M, Margulies DH. 2023. SARS-CoV-2 antibodies recognize 23 distinct epitopic sites on the receptor binding domain. Commun Biol 6:953.
39. Hamers-Casterman C, Atarhouch T, Muyldermans S, Robinson G, Hamers C, Songa EB, Bendahman N, Hamers R. 1993. Naturally occurring antibodies devoid of light chains. Nature 363:446-8.
40. Muyldermans S. 2021. Applications of Nanobodies. Annu Rev Anim Biosci 9:401-421.
41. Achour I, Cavelier P, Tichit M, Bouchier C, Lafaye P, Rougeon F. 2008. Tetrameric and homodimeric camelid IgGs originate from the same IgH locus. J Immunol 181:2001-9.
42. Rudolph MJ, Czajka TF, Davis SA, Thi Nguyen CM, Li XP, Tumer NE, Vance DJ, Mantis NJ. 2020. Intracellular Neutralization of Ricin Toxin by Single-domain Antibodies Targeting the Active Site. J Mol Biol 432:1109-1125.
43. Schubach WH, Mudri S, Dattwyler RJ, Luft BJ. 1991. Mapping antibody-binding domains of the major outer surface membrane protein (OspA) of Borrelia burgdorferi. Infect Immun 59:1911-5.
44. Haque HME, Mantis NJ, Weis DD. 2023. High-Throughput Epitope Mapping by Hydrogen Exchange-Mass Spectrometry. J Am Soc Mass Spectrom 34:123-127.
45. Jethva PN, Gross ML. 2023. Hydrogen Deuterium Exchange and other Mass Spectrometry-based Approaches for Epitope Mapping. Front Anal Sci 3.
46. Frye AM, Ejemel M, Cavacini L, Wang Y, Rudolph MJ, Song R, Mantis NJ. 2022. Agglutination of Borreliella burgdorferi by Transmission-Blocking OspA Monoclonal

bioRxiv preprint doi: https://doi.org/10.1101/2024.01.23.576890; this version posted January 24, 2024. The copyright holder for this preprint (which was not certified by peer review) is the author/funder, who has granted bioRxiv a license to display the preprint in perpetuity. It is made available under aCC-BY-NC-ND 4.0 International license.

Antibodies and Monovalent Fab Fragments. Infect Immun doi:10.1128/iai.00306-22:e0030622.

47. Gipson CL, de Silva AM. 2005. Interactions of OspA monoclonal antibody C3.78 with Borrelia burgdorferi within ticks. Infect Immun 73:1644-7.

48. Sadziene A, Thompson PA, Barbour AG. 1993. In vitro inhibition of Borrelia burgdorferi growth by antibodies. J Infect Dis 167:165-72.

49. Amcheslavsky A, Wallace AL, Ejemel M, Li Q, McMahon CT, Stoppato M, Giuntini S, Schiller ZA, Pondish JR, Toomey JR, Schneider RM, Meisinger J, Heukers R, Kruse AC, Barry EM, Pierce BG, Klempner MS, Cavacini LA, Wang Y. 2021. Anti-CfaE nanobodies provide broad cross-protection against major pathogenic enterotoxigenic Escherichia coli strains, with implications for vaccine design. Sci Rep 11:2751.

50. Lovrich SD, Callister SM, Schmitz JL, Alder JD, Schell RF. 1991. Borreliacidal activity of sera from hamsters infected with the Lyme disease spirochete. Infect Immun 59:2522-8.

51. Jiang W, Luft BJ, Munoz P, Dattwyler RJ, Gorevic PD. 1990. Cross-antigenicity between the major surface proteins (ospA and ospB) and other proteins of Borrelia burgdorferi. J Immunol 144:284-9.

52. Koide S, Yang X, Huang X, Dunn JJ, Luft BJ. 2005. Structure-based design of a second-generation Lyme disease vaccine based on a C-terminal fragment of Borrelia burgdorferi OspA. J Mol Biol 350:290-9.

53. Doering J, Van Slyke G, Donini O, Mantis NJ. 2022. Estimating Vaccine Potency Using Antibody-Based Competition Assays. Methods Mol Biol 2410:693-705.

54. Mukherjee J, Tremblay JM, Leysath CE, Ofori K, Baldwin K, Feng X, Bedenice D, Webb RP, Wright PM, Smith LA, Tzipori S, Shoemaker CB. 2012. A novel strategy for development of recombinant antitoxin therapeutics tested in a mouse botulism model. PLoS One 7:e29941.

55. Tremblay JM, Kuo CL, Abeijon C, Sepulveda J, Oyler G, Hu X, Jin MM, Shoemaker CB. 2010. Camelid single domain antibodies (VHHs) as neuronal cell intrabody binding agents and inhibitors of Clostridium botulinum neurotoxin (BoNT) proteases. Toxicon 56:990-8.

56. Vance DJ, Tremblay JM, Mantis NJ, Shoemaker CB. 2013. Stepwise engineering of heterodimeric single domain camelid VHH antibodies that passively protect mice from ricin toxin. J Biol Chem 288:36538-47.

57. Zuckert WR. 2007. Laboratory maintenance of Borrelia burgdorferi. Curr Protoc Microbiol Chapter 12:Unit 12C 1.

58. Samuels DS, Drecktrah D, Hall LS. 2018. Genetic Transformation and Complementation. Methods Mol Biol 1690:183-200.

bioRxiv preprint doi: https://doi.org/10.1101/2024.01.23.576890; this version posted January 24, 2024. The copyright holder for this preprint (which was not certified by peer review) is the author/funder, who has granted bioRxiv a license to display the preprint in perpetuity. It is made available under aCC-BY-NC-ND 4.0 International license.

629

630 **Tables**

631

Table 1. Anti-OspA V_HHs, families, epitope bins, binding affinities and agglutination activities

V_HH	Family	Bin	EC_{50} (nM)	K_D (nM)	k_{on} ($M^{-1}s^{-1}$)	k_{off} (s^{-1})	% Aggl
L8A1		3	>1000	N/A			-0.03
L8A4	L8H8	1	5.5	1.09	3.71E+05	4.03E-04	7.43
L8A9	L8A9	3	65.2	54.6	6.28E+04	3.43E-03	7.74 +/- 0.93
L8A10	L8A10	1	>1000	137	4.78E+04	6.54E-03	0.04
L8A12		3	850	99.7	1.53E+05	1.52E-02	1.6
L8B3			>1000	N/A			0.06
L8C2	L8A10	1	>1000	N/A			0.01
L8C3		3	24.8	8.82	2.28E+05	2.01E-03	12.59 +/- 2.33
L8D3	L8A10	1	35.4	10.4	1.14E+05	1.18E-03	0.28 +/- 0.49
L8D9		3	7.1	0.73	2.42E+04	1.76E-05	0.65 +/- 0.50
L8D10	L8H8	1	5.8	2.07	1.84E+05	3.82E-04	7.55
L8E1	L8H8	1	979	N/A			0.47
L8E3	L8C3	3	918	457	9.34E+04	4.27E-02	6.75
L8E9	L8A1	3	237	153	3.01E+04	4.60E-03	3.80
L8F2		3	381	152	4.74E+04	7.19E-03	4.33
L8F11			15.5	N/A			3.50
L8G1		3	133	16.4	1.98E+05	3.25E-03	7.56
L8G3	L8A9	3	220	50	6.63E+04	3.32E-03	6.21
L8G12		1	855	0.94	1.32E+05	1.24E-04	-0.03 +/- 0.05
L8H7		1	820	82.2	4.02E+04	3.30E-03	-0.02
L8H8	L8H8	1	1.8	0.28	1.54E+05	4.29E-05	10.12

N/A, no binding to rOspA detected by BLI; **Bold** indicates V_HHs expressed as Fc IgG fusion proteins (**Table 3**).

632

633

634

bioRxiv preprint doi: https://doi.org/10.1101/2024.01.23.576890; this version posted January 24, 2024. The copyright holder for this preprint (which was not certified by peer review) is the author/funder, who has granted bioRxiv a license to display the preprint in perpetuity. It is made available under aCC-BY-NC-ND 4.0 International license.

635

Table 2. OspA V_HH epitope mapping by HX-MS

V_HH	peptides[a]	2º struct.	Molar ratio[b]	HX time-course[c]
L8A4[d]	129-145, 148-157, 159, 161-171, 174, 175, 177	β-strands 10-14	4:1	screening
L8D10[d]	129-145, 148-157, 159, 161-171, 174, 175, 177	β-strands 10-14	4:1	screening
L8H8[d]	129-145, 148-157, 159, 161-171, 174, 175, 177	β-strands 10-14	4:1	complete
L8D3	148-157, 159, 161-171	β-strands 11-13	8:1	screening
L8G12	148-157, 159, 161-171, 174, 175, 177	β-strands 11-14	4:1	screening

[a], strongly protected peptides listed as OspA residue numbers (see supplementary information); [b], molar ratio V_HH:OspA; [c,] as described in (44); [d], derive from the same clonal family.

636

637

bioRxiv preprint doi: https://doi.org/10.1101/2024.01.23.576890; this version posted January 24, 2024. The copyright holder for this preprint (which was not certified by peer review) is the author/funder, who has granted bioRxiv a license to display the preprint in perpetuity. It is made available under aCC-BY-NC-ND 4.0 International license.

638

Table 3. Functional activity associated with monovalent (V_HH) and bivalent (VHH-Ig) OspA antibodies

		VHH	VHH-IgG1 Fc				
V_HH	**Bin**	**% Agg[a]**	**% Agg[a]**	**% Binding[b]**	**MFI[b]**	**%PI[+c]**	**CDK (nM)[d]**
L8D3	1	0.28 +/- 0.49	17.33 +/- 6.11	98.51 +/- 0.76	6894.89 +/- 425.76	2.23 +/- 0.47	2.5
L8G12	1	-0.03 +/- 0.05	18.02 +/- 6.48	98.23 +/- 1.05	6168.56 +/- 664.89	3.27 +/- 0.44	1.25
L8H8	1	10.12	20.70 +/- 4.88	96.26 +/- 0.92	5338.44 +/- 745.55	4.53 +/- 0.16	2.5
L8A9	3	7.74 +/- 0.93	21.99 +/- 2.28	97.39 +/- 1.75	5374.96 +/- 85.12	4.18 +/- 0.38	1.25
L8C3	3	12.59 +/- 2.33	25.25 +/- 1.25	96.57 +/- 2.38	7141.05 +/- 78.21	5.52 +/- 0.98	1.25
L8D9	3	0.65 +/- 0.50	16.47 +/- 4.57	98.46 +/- 0.80	4802.12 +/- 359.14	2.37 +/- 0.19	1.25

[a], Agglutination (%) with background subtracted, n=3 (except L8H8, n=1); [b], *B. burgdorferi* surface binding, n=2; [c], Propidium iodide positive cells, n=2; [d], Antibody-mediated, complement-dependent killing (CDK) assay are shown (EC_{50}) n=3. +/- values are standard deviations. By comparison, the EC_{50} values of 857-2 and LA-2 were 1.25 and ~0.75 nM, respectively.

639

640

641

642

643

644

645

bioRxiv preprint doi: https://doi.org/10.1101/2024.01.23.576890; this version posted January 24, 2024. The copyright holder for this preprint (which was not certified by peer review) is the author/funder, who has granted bioRxiv a license to display the preprint in perpetuity. It is made available under aCC-BY-NC-ND 4.0 International license.

646

647

648 **Figure Legends**

649

650 **Figure 1. V_HH recognition of recombinant OspA.** Expressed and purified V_HHs were tested
651 for binding to immobilized recombinant OspA ST1 by ELISA. V_HHs were grouped by clonal
652 relationships. (A) L8A1 family; (B) L8H8 family; (C) L8A9 family; (D) L8C3 family; (E)
653 L8A10 family; (F) "orphan" V_HHs not part of a clonal family.

654

655 **Figure 2. Assignment of V_HHs to OspA epitope bins.** Representative V_HH family members
656 (and all orphans) were tested for their ability to bind to rOspA that had been previously coated
657 by Bin 1-3 mAbs using BLI. A) Biotinylated-OspA was immobilized on Streptavidin coated
658 biosensors and then coated with mAbs from Bins 1-3 (top). Individual V_HHs were then allowed
659 to bind, and the change in the signal induced by the V_HHs is reported in each box. The data is
660 normalized to each V_HHs binding in the presence of bin 2 mAb 212-55, which did not block any
661 of the V_HHs from binding, and colorized so that dark purple represents strong
662 competition/inhibition and light green represents no competition. B) Surface representation of
663 OspA (PDB ID: 1OSP) (gray) colored with the HX-MS determined epitopes of the mAbs used in
664 panel A) colored blue, green, and shades of red for bins 1, 2 and 3, respectively.

665

666 **Figure 3**. **Mapping of V_HH epitopes of OspA by HX-MS.** The left hand column shows $\Delta\overline{HX}$
667 for each individual OspA peptide, arranged from N- to C-terminals of OspA. The dotted line
668 denotes the limit for statistically significant differences. The results were classified into
669 categories of protection, denoted by blue and cyan for protection (slower hydrogen exchange)
670 and yellow (faster hydrogen exchange) for the bound form of OspA relative to the free form. The
671 center and right-hand panels show the results mapped onto the surface and ribbon representations
672 of OspA (PDB ID: 1OSP).

673

674 **Figure 4. Surface labeling, agglutination and membrane permeability associated with OspA**
675 **V_HH-IgG.** Flow cytometry analysis of live *B. burgdorferi* strain B31 incubated with OspA V_HH-
676 IgG Fcs, where an Alexa 647 fluorescent-labeled anti-human IgG secondary antibody was used

bioRxiv preprint doi: https://doi.org/10.1101/2024.01.23.576890; this version posted January 24, 2024. The copyright holder for this preprint (which was not certified by peer review) is the author/funder, who has granted bioRxiv a license to display the preprint in perpetuity. It is made available under aCC-BY-NC-ND 4.0 International license.

677 to detect bound V_HH-IgG Fcs. (**Left panel**) Representative histogram analysis of *B. burgdorferi*
678 surface labeling by control and experimental MAbs. PB10 IgG and LA-2 IgG were used as
679 negative and positive controls, respectively. The geometric mean fluorescence intensity (gMFI),
680 and percent of positive events for Alexa 647 fluorescence are indicated. (**Right panel**)
681 Corresponding forward-scatter (FSC)/side-scatter (SSC) dot plots. The percent of events that are
682 agglutinated is indicated (black) and was calculated from the sum of events with increased FSC
683 and SSC, in the upper-left, upper-right, and lower-right quadrants, relative to total events
684 counted (20,000). The percent of events positive for PI staining, indicating membrane damage, is
685 shown in red.
686
687 **Figure 5. Complement-dependent borreliacidal activity imparted by V_HH-IgG Fc.** Reporter
688 strain GGW979 was mixed with serial dilutions of each V_HH-Fc IgG1 (A) Bin 1 and (B) Bin 2
689 diluted in phenol-free BSKII supplemented with gentamicin (40 μg/mL) and 20% human
690 complement. 857-2 and LA-2 IgG1 MAbs were included in each assay to serve as positive
691 controls for Bin 1 and Bin 3, respectively. Spirochete viability was measured 3 days later as
692 detailed in the Materials and Methods. Data are the results of three biological replicates with SD.
693 EC_{50} values were determined by the lowest dilution of antibody resulting in 50% reduction in
694 MFI relative to normalized controls.
695
696 **Figure 6. V_HH-IgG Fc recognition of OspA serotypes by ELISA.** (A) Amino acid alignment
697 of the seven OspA serotypes (ST1-7). Dots denote amino acid identity with ST1; one letter
698 amino acid codes shown in locations that differ from ST1. (**B**) Microtiter plates were coated with
699 indicated OspA serotypes (horizontal labels) or block solution only (control), then probed with
700 indicated Bin 1 (857-2, L8D3, L8G12, L8H8) or Bin 3 (LA-2, L8A9, L8C3, L8D9) antibodies
701 (vertical labels) and developed as described in the Materials and Methods. The heat map scale
702 (purple to green) is shown on the right and the numbers refer to absorbance values upon addition
703 of stop solution. Deep purple (0) represents no binding, while lighter green (4) represents strong
704 binding.

FIGURE 1

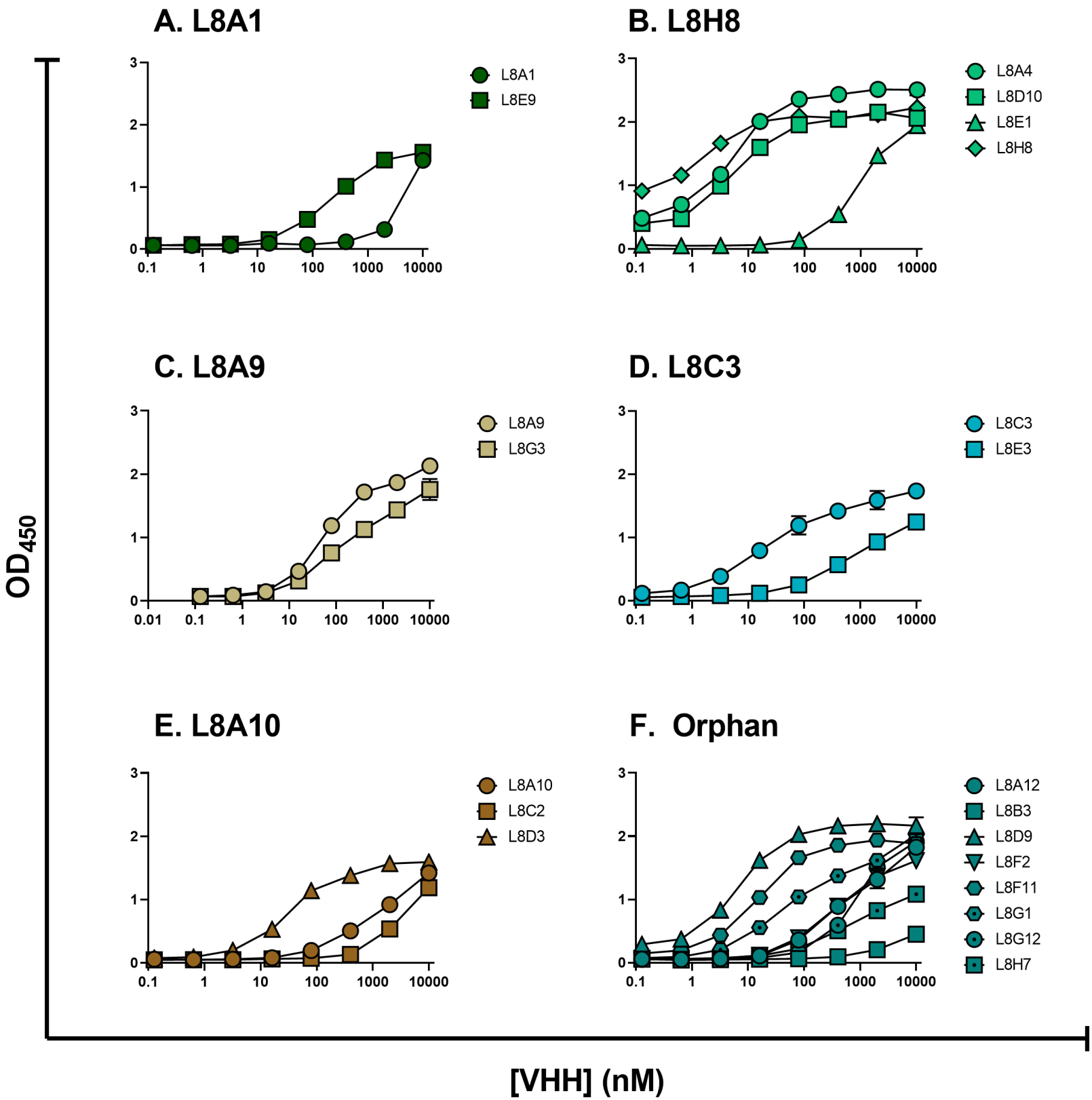
A. L8A1
L8A1
L8E9
B. L8H8
L8A4
L8D10
L8E1
L8H8
C. L8A9
L8A9
L8G3
D. L8C3
L8C3
L8E3
E. L8A10
L8A10
L8C2
L8D3
F. Orphan
L8A12
L8B3
L8D9
L8F2
L8F11
L8G1
L8G12
L8H7
OD450
[VHH] (nM)

FIGURE 2

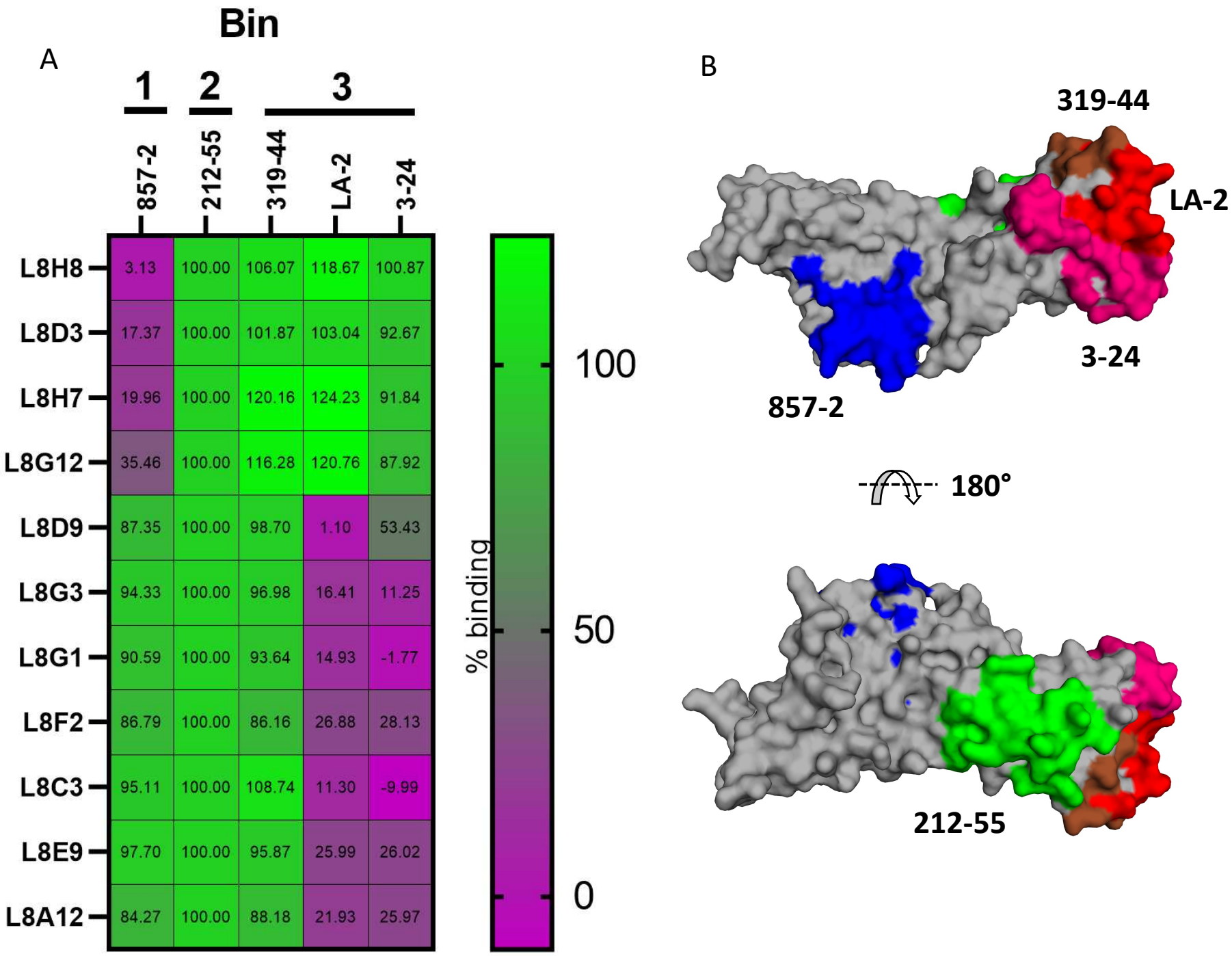
A
Bin
1
2
3
857-2
212-55
319-44
LA-2
3-24
L8H8 3.13 100.00 106.07 118.67 100.87
L8D3 17.37 100.00 101.87 103.04 92.67
L8H7 19.96 100.00 120.16 124.23 91.84
L8G12 35.46 100.00 116.28 120.76 87.92
L8D9 87.35 100.00 98.70 1.10 53.43
L8G3 94.33 100.00 96.98 16.41 11.25
L8G1 90.59 100.00 93.64 14.93 -1.77
L8F2 86.79 100.00 86.16 26.88 28.13
L8C3 95.11 100.00 108.74 11.30 -9.99
L8E9 97.70 100.00 95.87 25.99 26.02
L8A12 84.27 100.00 88.18 21.93 25.97
% binding
100
50
0
B
319-44
LA-2
3-24
857-2
180°
212-55

FIGURE 3

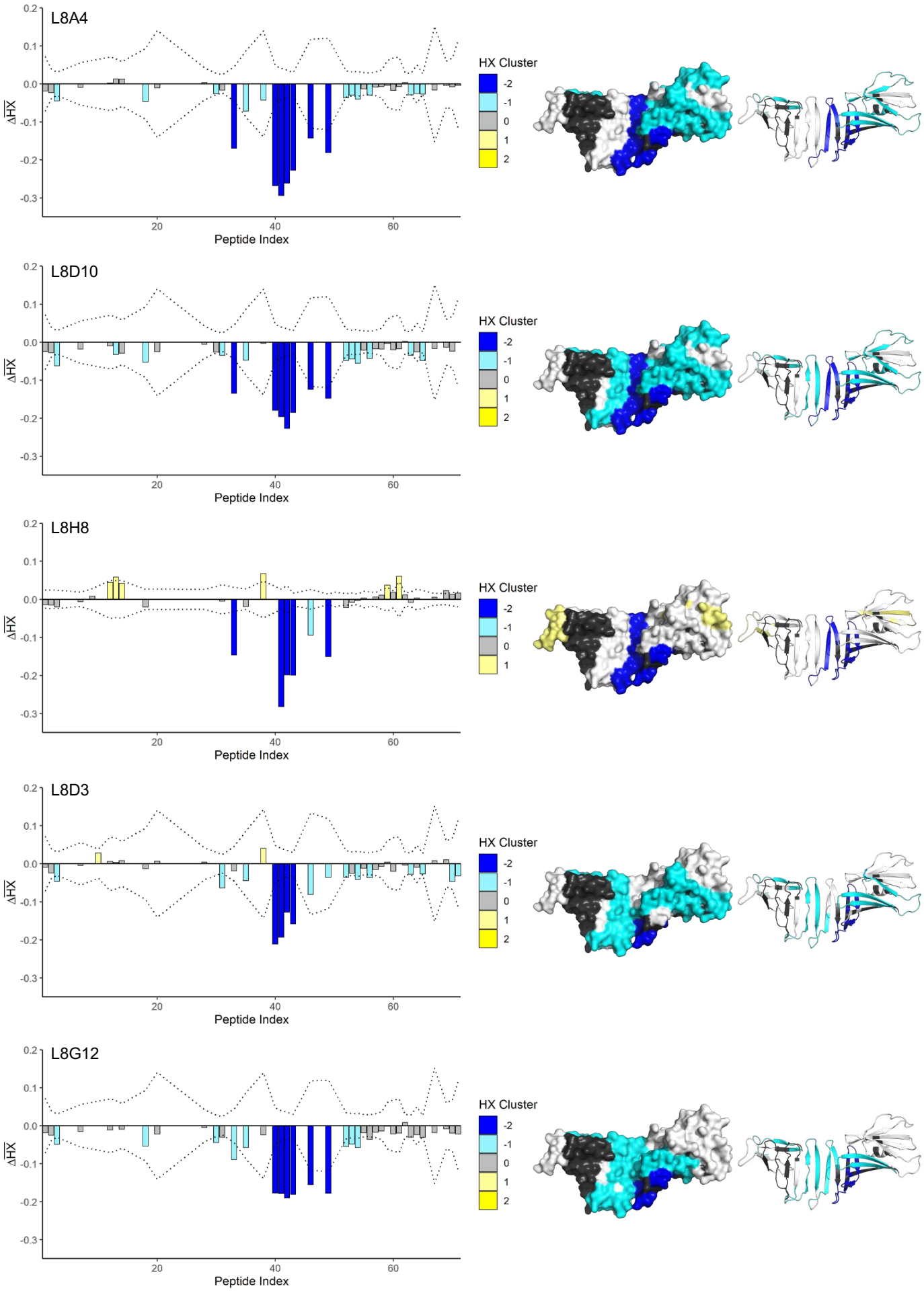
L8A4
L8D10
L8H8
L8D3
L8G12
ΔHX
Peptide Index
HX Cluster
-2
-1
0
1
2

FIGURE 4

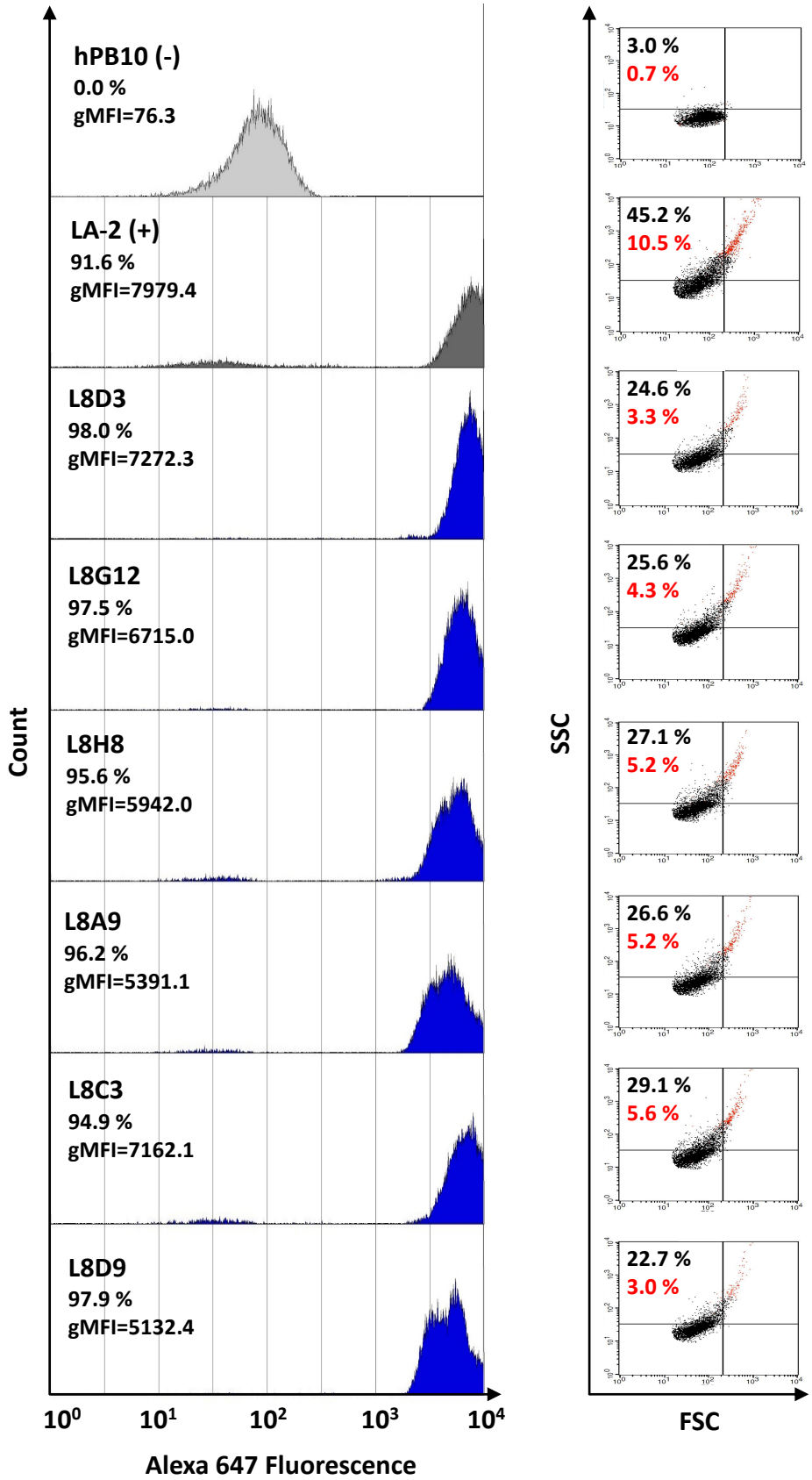
hPB10 (-)
0.0 %
gMFI=76.3
LA-2 (+)
91.6 %
gMFI=7979.4
L8D3
98.0 %
gMFI=7272.3
L8G12
97.5 %
gMFI=6715.0
L8H8
95.6 %
gMFI=5942.0
L8A9
96.2 %
gMFI=5391.1
L8C3
94.9 %
gMFI=7162.1
L8D9
97.9 %
gMFI=5132.4
Count
10^0 10^1 10^2 10^3 10^4
Alexa 647 Fluorescence
3.0 %
0.7 %
45.2 %
10.5 %
24.6 %
3.3 %
25.6 %
4.3 %
27.1 %
5.2 %
26.6 %
5.2 %
29.1 %
5.6 %
22.7 %
3.0 %
SSC
FSC

A. Bin 1

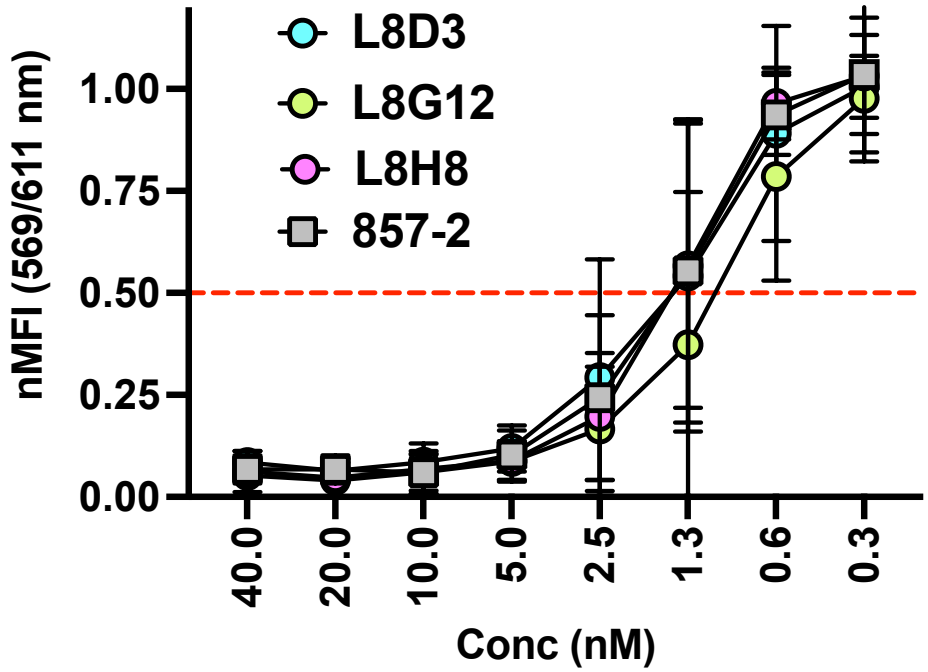
L8D3
L8G12
L8H8
857-2
nMFI (569/611 nm)
1.00
0.75
0.50
0.25
0.00
40.0
20.0
10.0
5.0
2.5
1.3
0.6
0.3
Conc (nM)

B. Bin 3

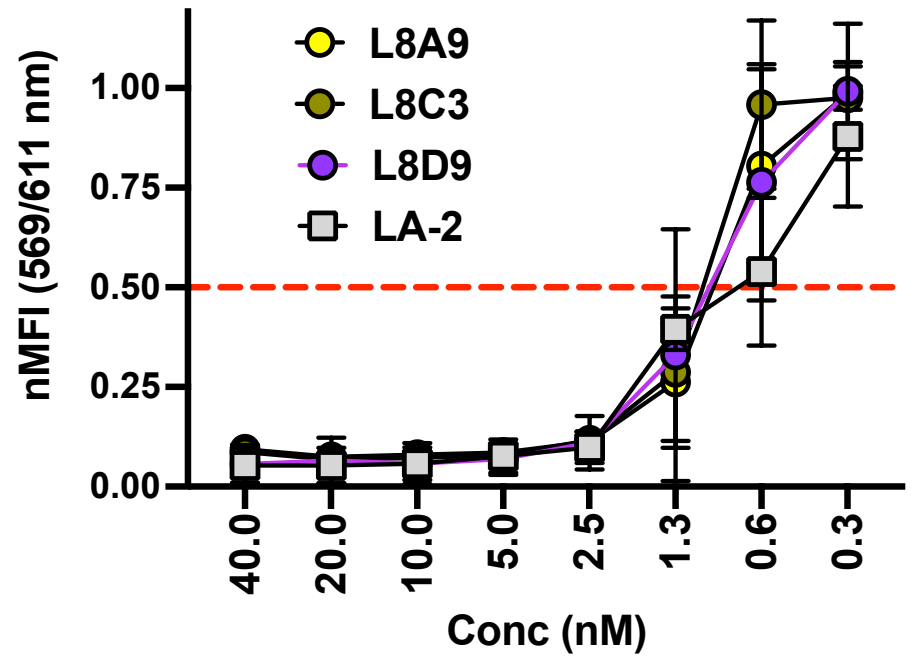
L8A9
L8C3
L8D9
LA-2
nMFI (569/611 nm)
1.00
0.75
0.50
0.25
0.00
40.0
20.0
10.0
5.0
2.5
1.3
0.6
0.3
Conc (nM)

FIGURE 6

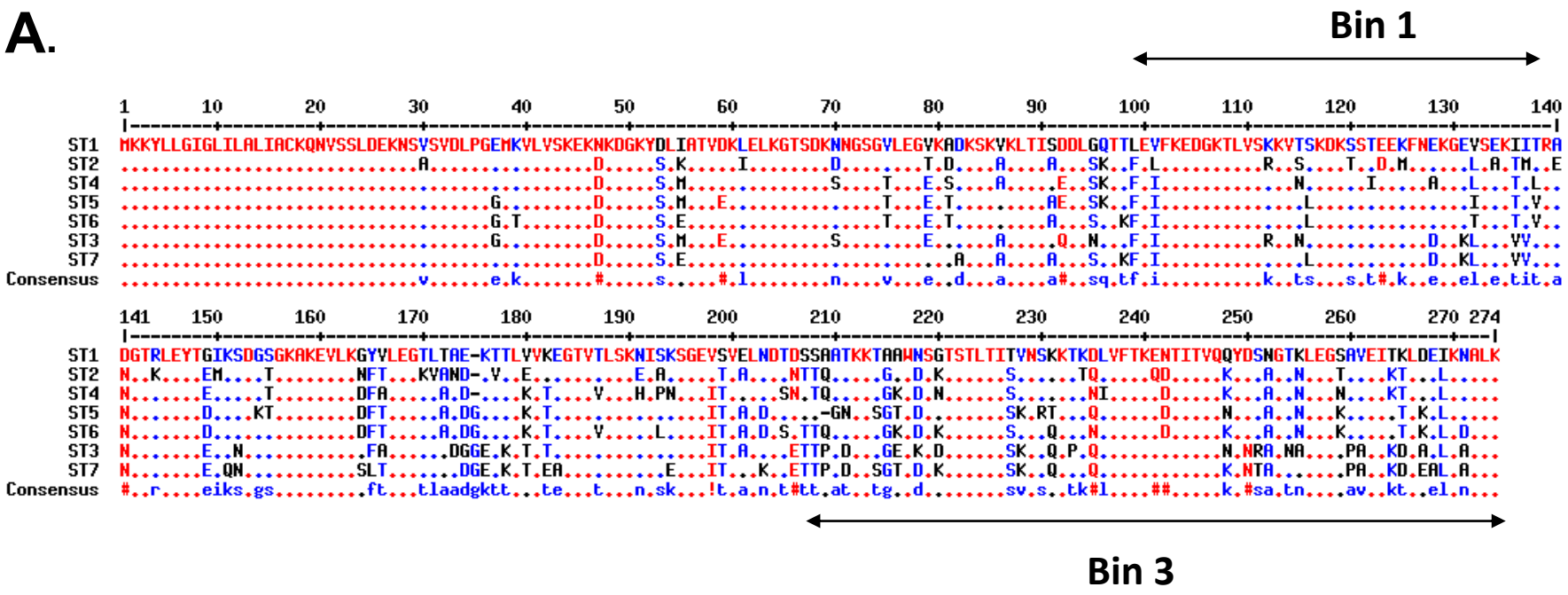
A.
Bin 1
Bin 3
ST1
ST2
ST4
ST5
ST6
ST3
ST7
Consensus

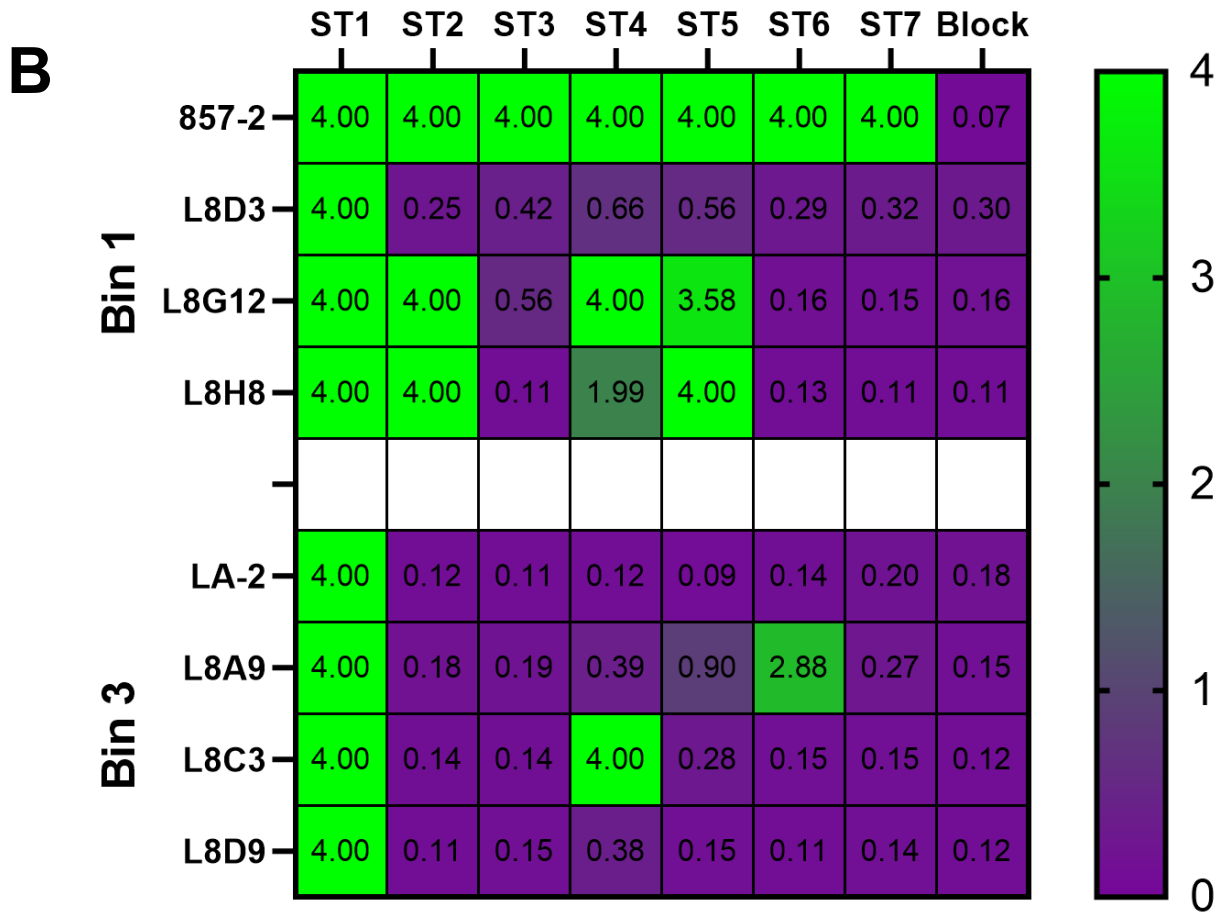
B
ST1 ST2 ST3 ST4 ST5 ST6 ST7 Block
Bin 1
857-2 4.00 4.00 4.00 4.00 4.00 4.00 4.00 0.07
L8D3 4.00 0.25 0.42 0.66 0.56 0.29 0.32 0.30
L8G12 4.00 4.00 0.56 4.00 3.58 0.16 0.15 0.16
L8H8 4.00 4.00 0.11 1.99 4.00 0.13 0.11 0.11
Bin 3
LA-2 4.00 0.12 0.11 0.12 0.09 0.14 0.20 0.18
L8A9 4.00 0.18 0.19 0.39 0.90 2.88 0.27 0.15
L8C3 4.00 0.14 0.14 4.00 0.28 0.15 0.15 0.12
L8D9 4.00 0.11 0.15 0.38 0.15 0.11 0.14 0.12
4
3
2
1
0